Original Article

Phenolic compounds prevent the oligomerization of α-synuclein and reduce synaptic toxicity

Ryoichi Takahashi[a], Kenjiro Ono[a], Yusaku Takamura[b], Mineyuki Mizuguchi[c], Tokuhei Ikeda[a,d], Hisao Nishijo[b], Masahito Yamada[a]*

Authors' affiliation

a. Department of Neurology and Neurobiology of Aging, Kanazawa University Graduate School of Medical Science, 13-1, Takara-machi, Kanazawa 920-8640, Japan.

b. System Emotional Science, Graduate School of Medicine and Pharmaceutical Science, University of Toyama, 2630, Sugitani, Toyama 930-0194, Japan.

c. Faculty of Pharmaceutical Sciences, University of Toyama, 2630, Sugitani, Toyama 930-0194, Japan.

d. Department of Neurology, National Hospital Organization Iou Hospital, Ni 73-1, Iwade-machi, Kanazawa 920-0192, Japan.

* **Corresponding author.** Masahito Yamada, Department of Neurology and Neurobiology of Aging, Kanazawa University Graduate School of Medical Science, 13-1 Takara-machi, Kanazawa, Ishikawa, 920-8640, Japan, Tel: +81-76-265-2290; Fax: +81-76-234-4253; E-mail: m-yamada@med.kanazawa-u.ac.jp

Running title: Phenolic compounds prevent αS oligomerization

***Keywords**:* α-synuclein, phenolic compounds, oligomerization, α-synucleinopathies, myricetin, rosmarinic acid

Abbreviations used: atomic force microscope, AFM; α-synuclein, αS; α-synuclein fibrils; fαS; circular dichroism spectroscopy, CD; curcumin, Cur; dementia with Lewy bodies, DLB; electron microscope, EM; epigallo catechin 3–gallate, EGCG; ferulic acid, FA; field excitatory postsynaptic potentials, fEPSPs; glutathione S-transferase, GST; Lewy body; LB; long-term potentiation, LTP; matrix-assisted laser desorption ionization time-of-flight mass, MALDI-TOF MS; 1-methyl-4phenyl-1,2,3,4-tetrahydropyridine, MPTP; myricetin, Myr; nordihydroguaiaretic acid, NDGA; nuclear magnetic resonance, NMR; Parkinson's disease, PD; photo induced cross-linking of unmodified proteins, PICUP; rosmarinic acid, RA; size-exclusion chromatography, SEC; sodium dodecyl sulfate-polyaclylamidegel electrophoresis, SDS-PAGE; thioflavin S, ThS; thioflavin T, ThT

Abstract

Lewy bodies, mainly composed of α-synuclein (αS), are pathological hallmarks of Parkinson's disease (PD) and dementia with Lewy bodies (DLB). Epidemiological studies showed that green tea consumption or habitual intake of phenolic compounds reduced PD risk. We previously reported that phenolic compounds inhibited αS fibrillation and destabilized preformed αS fibrils. Cumulative evidences suggest that low-order αS oligomers are neurotoxic and critical species in the pathogenesis of α-synucleinopathies. To develop disease modifying therapies for α-synucleinopathies, we examined effects of phenolic compounds (myricetin (Myr), curcumin, rosmarinic acid (RA), nordihydroguaiaretic acid, and ferulic acid) on αS oligomerization. Using the methods of photo induced cross-linking of unmodified proteins, circular dichroism spectroscopy, the electron microscope, and the atomic force microscope, we showed that Myr and RA inhibited αS oligomerization and secondary structure conversion. The nuclear magnetic resonance analysis revealed that Myr directly bound to the N-terminal region of αS, on the other hand, direct binding of RA to monomeric αS was not detected. Electrophysiological assays for long-term potentiation in mouse hippocampal slices revealed that Myr and RA ameliorated αS synaptic toxicity by inhibition of αS oligomerization. These results suggest that Myr and RA prevent αS aggregation process and reduce the neurotoxicity of αS oligomers.

Introduction

Parkinson's disease (PD), dementia with Lewy bodies (DLB), and multiple system atrophy (MSA) belong to the category of α-synucleinopathies. PD is characterized by the loss of nigrostriatal dopaminergic neurons associated with motor impairment, and the main symptoms of PD are muscle rigidity, resting tremor, bradykinesia, and postural instability (Jankovic 2008). In PD, neurodegenerative lesions with Lewy bodies (LBs) are distributed mainly in the dopaminergic neurons of the substantia nigra, and also in other brain stem and limbic regions (Braak *et al.* 2004). DLB is a disorder of progressive dementia characterized by fluctuation in mental decline, visual hallucination, parkinsonism, and widespread distribution of LBs in the brain (McKeith *et al.* 2005). LBs are the accumulation of intracellular inclusions of the insoluble protein, which are mainly composed of α-synuclein (αS), and are pathological hallmarks of diseases known as PD and DLB (McKeith *et al.* 2005; Spillantini *et al.* 1998).

αS is a neuronal presynaptic protein, involved in vesicular trafficking, neurotransmitter release, and regulation of neurotransmission (Clayton and George 1999; Fujiwara *et al.* 2002). The monomeric αS is natively unfolded soluble protein without well-defined secondary or tertiary structures (Weinreb *et al.* 1996), but it transforms into cross-β-sheet rich amyloid by self-assembly at physiological conditions via partially folded intermediates and soluble oligomers (Uversky *et al.* 2001). While the intimate origin for the αS toxicity is yet to be unclear, accumulated evidences suggest that oligomeric forms of αS, rather than the larger intracellular inclusions, might be more bioactive and, possibly, cytotoxic, causing not only neuronal dysfunction but cell death (Martin *et al. 2012*; Winner *et al.* 2011).

Epidemiological studies showed an inverse relationship between green tea consumption and the risk of developing PD (Ascherio *et al.* 2001; Chan *et al.* 1998). The major polyphenols present in green tea are catechins, especially epigallo catechin 3-gallate (EGCG), and green tea contains more myricetin (Myr) compared with black tea (Bosetti *et al.* 2005). Recently, a prospective study showed habitual intake of some polyphenols may reduce PD risk, and the association was more pronounced in men than women (Gao *et al.* 2012).

Evidences of *in vitro* and *in vivo* studies have indicated the protective effects of polyphenols, such as EGCG in green tea, curcuminoids in curry, baicalein extracted from the root of *Scutellaria baicalensis*, a traditional Chinese herb, or extracts from grape and blueberry, against neuronal damage in PD (Chao *et al.* 2012; Masuda *et al.* 2006). Levites *et al.* reported the neuroprotective activity of EGCG on 1-methyl-4-phenyl-1,2,3,4-tetrahydropyridine (MPTP)-induced parkinsonism in animal models (Levites *et al.* 2001). It is suggested that the neuroprotective effects of EGCG are mediated by iron-chelating activities and free-radical-scavenging activities possessed by the cathecol group (Weinreb *et al.* 2009). Polyphenols also have protective effects against αS toxicity (Liu *et al.* 2011; Jiang *et al.* 2013). In PD cell model experiments, Curcumin (Cur) reduced αS induced cytotoxicity by reduction of intracellular reactive oxygen species, mitochondrial depolarization, cytochrome c release, and caspase-9 and caspase-3 activation (Liu *et al.* 2011), or downregulation of mTOR/p70S6K signaling and the recovery of macroautophagy (Jiang *et al.* 2013).

We showed that phenolic compounds such as the wine-related polyphenol Myr, a major component of curry spice turmeric Cur, rosmarinic acid (RA), nordihydroguaiaretic acid (NDGA), and ferulic acid (FA) inhibited the formation of αS fibrils (fαS), as well as destabilized preformed fibrils (Ono and Yamada 2006). Similarly, it was reported that baicalein (Zhu *et al.* 2004) and EGCG (Bieschke *et al.* 2010; Ehrnhoefer *et al.* 2008) also inhibited fαS formation and destabilized preformed fαS.

Given this background, we examined the ability of five phenolic compounds, Myr, FA, NDGA, Cur, and RA (Fig.1), to interact with αS and to inhibit the oligomerization of αS using well-established biophysical techniques. We assessed the oligomerization of αS with the methods of photo induced cross-linking of unmodified proteins (PICUP), sodium dodecyl sulfate-polyaclylamidegel electrophoresis (SDS-PAGE), circular dichroism spectroscopy (CD), electron microscope (EM), atomic force microscope (AFM), and nuclear magnetic resonance (NMR) (Bitan and Teplow 2004; Ono *et al.* 2008; Ono and Yamada 2011). We also evaluated the seeding effect of oligomeric αS using thioflavin S (ThS) assay (LeVine 1993; Naiki and Nakakuki 1996; Ono *et al.* 2013). Finally, we examined whether the phenolic compounds reduced αS oligomers-induced synaptic dysfunction with electrophysiological assays for long-term potentiation (LTP).

Materials and methods

Chemicals and reagents

Chemicals were obtained from Sigma-Aldrich (St. Louis, MO, USA) and were of the highest purity available. Water was produced using a Milli-Q system (Nihon Millipore K.K., Tokyo, Japan).

Proteins and phenolic compounds

αS peptides were obtained from r-peptide (Osaka, Japan), and were >95% purity. Purified peptides were stored as lyophilizates at -20°C. To prepare peptides for study, αS peptide lyophilizates were dissolved at a nominal concentration of 50 μM in 20 mM Tris HCl buffer, pH 7.4. The peptide solution was centrifuged for 30 min at 16,000 ×*g* at 4°C. A stock solution of glutathione S-transferase (GST; ~26 kDa) (Sigma-Aldrich) was prepared by dissolving the lyophilizate to a concentration of 250 μM in 60 mM NaOH. Prior to use, aliquots were diluted 10-fold into 20 mM Tris-HCl, pH 7.4. We examined 5-phenolic compounds such as Myr, FA, NDGA, Cur, and RA. They were dissolved in ethanol to a final concentration of 2.5 mM and then diluted with 20 mM Tris HCl buffer, pH7.4, to produce concentrations 5, 10, 25, 50, 100, and 500 μM for CD, PICUP, and AFM as described previously (Bitan and Teplow 2004; Ono *et al.* 2012a).

Circular dichroism spectroscopy

CD spectra of αS compound mixtures were acquired immediately after sample preparation or following 1-5 days of incubation. CD measurements were made by removing a 200-μL aliquot from the reaction mixture, adding the aliquot to a 1-mm path length CD cuvette (Hellma, Forest Hills, NY), and acquiring spectra in a J-805 spectropolarimeter (JASCO, Tokyo, Japan). The CD curettes were maintained on ice prior to introduction into the spectrometer. Following temperature equilibration, spectra were recorded at 22°C from ~190-260 nm at 0.2 nm resolution with a scan rate of 100 nm/min. Ten scans were acquired and averaged for each sample. Raw data were manipulated by smoothing and subtraction of buffer spectra according to the manufacturer's instructions.

Chemical cross-linking and determination of oligomer frequency distributions

Immediately after their preparation, samples were cross-linked using PICUP, as described (Ono *et al.* 2012b). Briefly, to 18 μM of 50 μM protein solution were added

1 μL of 4 mM tris(2,2'-bipyridyl)dichlororuthenium(II) (Ru(bpy)) and 1 μL of 80 mM ammonium persulfate. The final protein of αS : Ru(bpy) : ammonium persulfate molar ratios were 1 : 4 : 80. The mixture was irradiated for 1 s with visible light, and then the reaction was quenched with 2 μL of 1 M DTT (Invitrogen) in ultrapure water. Determination of the frequency distribution of monomers and oligomers was accomplished using SDS-PAGE and silver staining as described (Ono *et al.* 2012b). Briefly, 8 μL of each cross linked sample was electrophoresed on a 10-20% gradient tricine gel and visualized by silver staining (Invitrogen). Uncross-linked samples were used as controls in each experiment. Densitometry was performed with a luminescent image analyzer (LAS 4000 mini, Fujifilm, Tokyo, Japan) and image analysis software (Multi gauge, version 3.2, Fujifilm). The intensity of each band in a lane from the SDS gel was normalized to the sum of the intensities of all the bands in that lane according to the formula, ▯▯=▯▯/▯=1▯▯▯×100 (%), where R_i is the normalized intensity of band I, and I_i is the intensity of each band i. R_i varies from 0-100. To calculate the oligomer ratio, the sum of oligomers intensities of αS with 2.5, 5, 25, 50, and 250 μM Myr, FA, NDGA , Cur, or RA, respectively, was divided by the sum of oligomer intensities without each compound. The EC_{50} was defined as the concentration of phenolic compounds to inhibit α synuclein oligomerization to 50% of the control value. The EC_{50} was calculated by sigmoidal curve fitting, using GraphPad Prism software (version 4.0a, GraphPad Software, Inc.).

Size-exclusion chromatography

PICUP reagents and phenolic compounds were removed from cross-linked samples by size-exclusion chromatography (SEC) as described previously (Ono *et al.* 2012a; Volles *et al.* 2001). To do so, we used the Superdex 200 10/300 GL column (GE healthcare, Tokyo, Japan). At first, the column was washed twice with 0.5 M NaOH. Two hundred μL of cross-linked sample was then loaded. The column was eluted with 20 mM Tris HCl buffer at a flow rate of 0.5 mL/min. The first 4 mL of elute was collected. Fractions were lyophilized immediately after collection.

Seeding activity of assemblies of αS

For the seeding assay, uncross-linked αS or cross-linked αS with or without Myr and RA at a concentration of 25 μM in 20 mM Tris buffer, pH 7.4 were added as seeds to uncross-linked αS at a ratio of 10% (v/v). The mixtures were incubated at 37°C for 0-7 days. ThS fluorescence were measured as mentioned below at 0, 1, 2, 6, 24. 48, 72, 96, 120, 144, and 168 hrs. Before the seeding assay, secondary structure of each αS assembly was checked, using CD studies.

Thioflavin S binding

Thioflavin binding assays were performed because fluorescence intensities do correlate with αS fibril content (LeVine 1993; Naiki and Nakakuki 1996). The reaction mixture contained 5 μM ThS (MP Biomedicals, Irvine, CA, USA) and 50 mM glycine-NaOH buffer, pH 8.5. After brief vortexing, fluorescence was determined three times at intervals of 10 s using a Hitachi F-7500 fluorometer (Hitachi, Tokyo, Japan). Excitation and emission wavelength of 440 and 521 nm were used for αS assay, respectively. Fluorescence was determined by averaging three readings and subtracting the ThS blank readings.

Electron microscope

A 10-μL aliquot of each sample was spotted onto a glow-discharged, carbon-coated formvar grid (Okenshoji, Co, Ltd, Tokyo, Japan) and incubated for 20 minutes. The droplet then was displaced with an equal volume of 2.5% (v/v) glutaraldehyde in water and incubated for an additional 5 minutes. Finally, the peptide was stained with 8 μL of 1% (vol/vol) filtered (0.2 μm) uranyl acetate in water (Wako Pure Chemical Industries, Ltd, Osaka, Japan). This solution was wicked off and then the grid was air-dried. The samples were examined using a JEM-1210 transmission EM (JEOL Ltd., Tokyo, Japan).

Atomic force microscope

Peptide solutions were characterized using a Nanoscope IIIa controller (Veeco Digital

Instruments, Santa Barbara, CA, USA) with a multimode scanning probe microscope equipped with a JV (J-type vertical) scanner. All measurements were carried out in the tapping mode under ambient conditions using single-beam silicon cantilever probes. A 10-μL aliquot of each sample was spotted onto freshly cleaved mica (Ted Pella, Inc., Redding, CA, USA), incubated at room temperature for 5 minutes, rinsed with water, and then blown dry with air. At least 4 regions of the mica surface were examined to confirm the homogeneity of the structures throughout the sample. Mean particle heights were analyzed by averaging the measured values of 8 individual cross-sectional line scans from each image only when the particle structure was confirmed.

Electrophysiology

The field excitatory postsynaptic potentials (fEPSPs) were recorded from the CA1 region of acute hippocampal slices derived from C57BL/6 mice (male, 4-5 weeks of age). The procedures for slice preparation and electrophysiological recording were described previously (Takamura *et al.* 2014). Briefly, 300-μm thick transverse hippocampal slices were placed in a physiological chamber perfused with artificial cerebrospinal fluid (125 mM NaCl, 3.5 mM KCl, 1.25 mM NaH_2PO_4, 25 mM $NaHCO_3$, 2.0 mM $MgSO_4$, 2.0 mM $CaCl_2$, and 20 mM glucose and aerated with a mixture of 95% O_2 and 5% CO_2) at a rate of 1 mL/min at 30°C. Shaffer collaterals/commissural bundle in the CA3 hippocampal subfield were stimulated using a bipolar stainless steel wire electrode at 20-s intervals throughout the experiment. The fEPSPs were recorded from the stratum radiatum in the CA1 hippocampal subfield using a sharp glass electrode (2-6 Mohms, filled with 2 M NaCl). After fEPSP baseline became stabilized, slice was incubated with circulation of 10 ml αS sample (1 μM) for 90 min on the experimental chamber without electric stimulation. fEPSP recording was restarted after incubation and confirmed baseline stability at least 20 min. LTP was induced by two train of tetanic stimulation delivered at 100 Hz for 1 s. The evoked potential was amplified (×1000), filtered (0.1-1000Hz), digitized (20 kHz), and stored in a computer for off-line analysis using the PowerLab system (AD Instruments, Colorado Springs, CO). LTP values were presented as the percentage of average fEPSPs slope relative to the mean value of the base line before tetanic stimulation.

NMR spectroscopy

The synthetic DNA encoding human αS was inserted into pOPTH plasmid. Sequencing of the inserted DNA was performed on an ABI PRISM 3130 Genetic Analyzer (Applied Biosystems). The αS protein with an N-terminal His-tag (MAHHHHHH) was expressed in *E. coli* BL21(DE3) harboring the pOPTH plasmid. The cells were grown in M9 minimal medium supplemented with $^{15}NH_4Cl$ and ^{13}C-glucose. Purification of αS was done with a Ni-NTA agarose resin (QIAGEN), followed by further purification by gel-filtration on a Superdex 75 16/60 column (GE

Healthcare Bio-Sciences). Matrix-assisted laser desorption ionization time-of-flight mass (MALDI-TOF MS) analysis showed that His-tagged αS has no methionine at the N-terminus. MALDI-TOF MS analysis was performed on a Bruker Daltonics Autoflex-T1 mass spectrometer.

Stock solutions of Myr and RA (54 mM) were prepared by dissolution in dimethylsulfoxide. Aliquots of the phenolic solutions were mixed with a solution containing 41 μM $^{13}C/^{15}N$-synuclein, 10 mM HEPES (pH 7.4), 50 mM NaCl, 90 μM NaN_3, 90 μM 2,2-dimethyl-2-silapentane-5-sulfonate sodium salt and 10% D_2O. The polyphenol concentration was 0.41 mM so that the final αS : polyphenol concentration ratio was 1 : 10. An NMR sample of the αS alone was also prepared in the same manner without polyphenol. The NMR sample was incubated at 15°C for 6 days before NMR measurements. All NMR spectra were obtained at 15°C with a Bruker Avance 800 MHz spectrometer equipped with a cryoprobe (Bruker BioSpin, Rheinstetten, Germany). NMR data were processed with NMRPipe (Delaglio *et al.* 1995) and analyzed with NMRView (Johnson. 2004). The published backbone resonance assignments of αS (BMRB Entry 16300) were transferred to the data of His-tagged αS without polyphenol (Rao *et al.* 2009). The transferred assignments were confirmed by analyzing CBCANH, CBCA(CO)NH, HNCO and HN(CA)CO (Clubb *et al.* 1992; Grzesiek and Bax 1992a; Grzesiek and Bax 1992b; Grzesiek and Bax 1993).

NMR-based molecular modeling

The model of αS was obtained with the use of CS-ROSETTA and the chemical shift assignment data (Rao *et al.* 2009; Shen *et al.* 2008; Shen *et al.* 2009). CS-ROSETTA generated the ensemble of the disordered αS, and one of them was used to show the regions affected by the polyphenol-binding. Figure depicting the αS model were prepared with the program PyMOL (DeLano Scientific, New York, USA).

Statistical analysis

Dunnett multiple comparisons were used to determine statistical significance between cross-linked αS group versus other groups in LTP analysis. These tests were implemented within GraphPad Prism software (MDF, Tokyo, Japan). Significance was defined as $p < 0.05$.

Results

αS oligomerization

To determine whether the five phenolic compounds blocked formation of low n-order αS oligomers, we used PICUP, a photochemical cross-linking method that is rapid, efficient, requires no structural modification of αS, and accurately reveals the oligomerization state of αS (Bitan and Teplow 2004). Following cross-linking as reported previously (Ono *et al.* 2012b), αS existed predominately as a mixture of monomers and oligomers of order 2-4, and higher order oligomers appear as smear bands (Fig. 2A). When 25 μM Myr was mixed with αS at a peptide : compound ratio of 1 : 1, oligomerization was blocked, bands of tetramer and higher order oligomers disappeared, and intensity of trimer band was decreased (Fig. 2A). When 250 μL of Myr was mixed with αS at a peptide : compound ratio of 1 : 10, oligomerization was blocked almost completely (Fig. 2A). When 25 (1 : 1) or 250 μM (1 : 10) RA was mixed with αS at the same ratios as used above, comparable effects were observed on αS oligomerization (Fig. 2A).

With αS : FA at a 1 : 1 ratio, intensities of bands of tetramer and higher order oligomers were decreased (Fig. 2A). At a higher concentration of FA (αS : FA, 1 : 10), oligomerization was blocked almost completely. With αS : NDGA at a 1 : 1 ratio and 1 : 10 ratio, similar effects was observed on αS oligomerization (Fig. 2A). With αS : Cur at a 1 : 1 ratio, no inhibition of αS oligomerization was observed. With αS : Cur at a 1 : 10 ratio, tetramer band was disappeared, and intensity of trimer band was decreased.

The results indicated that Myr and RA had the stronger inhibitory effects on αS oligomerization, compared to FA, NDGA, and Cur. We confirmed dose dependence of inhibitions by Myr and RA (Fig. 2, C and D). The EC_{50} of Myr and RA for the αS oligomerization were 23.9 and 22.7 μM, respectively.

A potential problem relates to the possibility that the inhibition of αS oligomerization could have resulted from an alternative compound, which may form from a possible side reaction of the inhibitor and the PICUP sensitizer. To evaluate this possibility, cross-linking reactions also were performed on GST, a positive control for the cross-linking chemistry (Fancy and Kodadek 1999). Uncross linked GST exhibited an intense monomer band and a relatively faint dimer band (Fig. 2B). Cross-linking produced an intense dimer band, which was expected because GST exists normally as a homodimer, as well as higher-order cross-linked species. No alterations in GST cross-linking were observed in the presence of Myr, FA, NDGA, Cur, or RA at either of the two protein : compound ratios tested, 1 : 1, 1 : 10. Thus, the significant inhibition of αS oligomerization is from a direct interaction with the phenolic compounds.

Size-exclusion chromatography

The waves of SEC were shown in Figure S1A. Reconstitution of the lyophilizates to a nominal concentration of 25 μM in 20 mM Tris HCl buffer, pH 7.4, followed by SDS-PAGE analysis, showed that removal of reagents and phenolic compounds, lyophilization and reconstitution did not alter the oligomer composition of any of the peptide populations under study (Figure S1B).

αS assembly morphology

We used AFM and EM to determine the morphology of the small assemblies present following PICUP of αS with or without phenolic compounds. The height of uncross-linked αS was 0.53 ± 0.05 nm (Fig. 3 and Table 1) from AFM analysis. Following PICUP, the height of αS oligomers became 1.60 ± 0.24 nm. These morphologies are consistent with our previous findings (Ono *et al.* 2011; Ono *et al.* 2012b). When αS was cross-linked with Myr at a compound : peptide ratio of 1 : 2, the height of treated αS decreased to 0.58 ± 0.06 nm. When αS was cross-linked with RA at a compound : peptide ratio of 1 : 2, the height of treated αS was decreased to 0.57 ± 0.06 nm (Fig. 3 and Table 1). Similarly, when αS was cross-linked with NDGA, FA, or Cur at a compound : peptide ratio of 1 : 2, the height of treated αS decreased to 0.54 ± 0.06 nm, 0.57 ± 0.07 nm, or 0.60 ± 0.07 nm, respectively.

Similar data were obtained from EM analysis. The diameter of uncross-linked αS was 2.32 ± 0.17 nm. Following PICUP, the diameter of αS oligomers became 11.94 ± 1.51 nm. These morphologies are also consistent with our previous findings (Ono *et al.* 2012b). When αS was cross-linked with Myr, NDGA, FA, Cur, or RA at a compound : peptide ratio of 1 : 2, the diameters of treated αS decreased to 2.80 ± 0.34 nm, 2.70 ± 0.27 nm, 2.99 ± 0.38 nm, 3.15 ± 0.38 nm, or 2.67 ± 0.35 nm, respectively (Table 1).

αS secondary structure dynamics

The above oligomerization studies revealed effects of the phenolic compounds at the initial stages of peptide self-association. To examine whether the phenolic compounds altered the secondary structure of the αS, we undertook CD studies (Fig. 4). αS, incubated alone, produced initial spectra characteristic of statistical coils (Fig. 4A). The major feature of these spectra was a large magnitude minimum centered at ~198 nm. αS displayed substantial secondary structure changes between days 2-3 that were consistent with the previous study (Ono *et al.* 2012b). When αS were incubated with Myr and RA at a compound : peptide ratio of 1 : 2, no such transitions were observed (Fig. 4, B and C).

Secondary structures of αS assembly

We measured secondary structure of seeds, such as uncross-linked αS, cross-linked αS with or without Myr or RA, using CD studies. The seed of cross-linked αS without phenolic compounds produced spectrum characteristic of β-sheet, on the other hand, the seeds of uncross-linked αS and cross-linked αS with Myr or RA produced spectrum characteristic of statistical coils (Figure S2A).

Seeding activities of αS assemblies

αS fibril assembly proceeds along a nucleation-dependent polymerization process (Wood et al. 1999). To monitor the abilities of cross-linked αS with or without phenolic compounds to exert fibril formation as seeds, we measured the time dependence of ThS fluorescence in seeded fibril formation experiments (Figure S2B). Uncross-linked αS displayed a quasisigmoidal process curve characterized by an ~6 hr lag time, an ~96 hr period of increasing ThS binding, and a binding plateau occurring after ~120 hr (Figure S2B). The unseeded reaction did not display initial fluorescence increase, within experimental error. Adding 10% cross-linked αS oligomers eliminated the lag period and produced a quasihyperbolic increase in fluorescence that reached maximal levels at ~48 hr, suggesting that cross-linked αS oligomers functioned as seeds. However, this seeding activity had disappeared in the cross-linked αS with Myr or RA (Figure S2B). Maximal ThS levels for the αS oligomers seeded reaction was reached in 72 hr, whereas those of seeded with uncross-linked αS, and cross-linked αS with Myr or RA reached in 120 hr.

Electrophysiology

To obtain an index of cross-linked αS-induced functional alteration of synaptic transmission, we analyzed LTP in the CA1 region of mouse hippocampal slices. Synaptic current strength was estimated from fEPSP slope (Fig. 5). The vehicle group indicated LTP by tetanus stimulation (166 ± 7.6%). Uncross-linked αS did not affect LTP (177 ± 15.5%). Cross-linked αS completely inhibited induction of LTP (87 ± 19.4%). In contrast, cross-linked αS treated with Myr and RA induced LTP comparable with that in the vehicle (150 ± 15.6% and 155 ± 18.1%, respectively). Fig. 5 shows differences in LTP induction among the five treatment groups. There was a significant group effect on %fEPSP slope in the cross-linked αS group was significantly lower than those in the other four groups, indicating that cross-linked αS induced LTP suppression, but cross-linked αS treated with Myr and RA did not.

NMR studies

In order to study the interaction between the phenolic compounds and αS, we utilized NMR spectroscopy, a widely accepted method to obtain atomic level aspects of protein structure and ligand binding. Fig. 6 shows the overlaid ^{1}H-^{15}N HSQC spectra of the αS alone and the αS containing the phenolic compounds at 1 : 10 molar ratio (αS : polyphenol). The ^{1}H-^{15}N HSQC spectra of αS are typical of an unstructured protein with limited resonance dispersion in the proton dimension (Wu et al. 2008).

Myr causes the reduction in the signal intensities due to the broadening of NMR resonances (Fig. 6A). The broadening results from the interactions between Myr and αS. Severe broadening was observed only within the first nine residues of αS, indicating that the N-terminal region was involved in the Myr-binding (Fig. 6A). On the other hand, neither chemical shift changes nor line broadening was observed upon RA addition, suggesting that RA did not bind to monomeric αS (Fig. 6B).

Discussion

We previously reported that several antioxidants including the phenolic compounds, Myr, FA, NDGA, Cur, and RA, had the inhibitory effects on αS fibrillization and αS fibril–destabilizing effect (Ono *et al.* 2003). In this study, we revealed that all five phenolic compounds had dose-dependently inhibitory effects on αS oligomerization, using the PICUP studies. Using EM and AFM analysis, the diameters and the heights of cross-linked αS treated with phenolic compounds were smaller than cross-linked αS oligomers. The CD studies unraveled that Myr and RA stabilized αS populations comprising mostly random coil and inhibited statistical coils → β-sheet conversion. In ThS assay, cross-linked αS treated with Myr and RA lost seeding activities. Taken together, we revealed that the abilities of Myr and RA to inhibit αS oligomerization and secondary structure conversion. To unravel chemical and neurophysiological basis for these effects, we performed LTP experiment and NMR analysis. Myr and RA decreased synaptic toxicities induced by αS oligomers on LTP assay of hippocampal slices. NMR showed the direct binding of Myr to the first nine residues of the N-terminal region of the monomeric αS protein, on the other hand, the direct binding of RA to the αS monomer was not detected.

What is the mechanism underlying the inhibitory effects of the phenolic compounds on αS oligomerization? The binding of Myr to the first nine residues of the N-terminus of αS in the NMR experiment might contribute to inhibition of αS oligomerization. The sequence of αS can be divided into three domains: the N-terminal domain, the central fragment, also known as NAC (non-amyloid β component) region, and the C-terminal region. NAC region (residues 61-95) was reported to represent the critical determinant of the oligomerization and the fibrillation process of αS (Hejjaoui *et al.* 2012). The C-terminal region (residues 96-140) is highly disordered and negatively charged, and it was shown that negatively charged side chains located in C-terminal region of αS acted to retard fibril formation by thioflavin T (ThT) binding assay (Izawa *et al.* 2012). Similar to Myr, a small molecular tweezer, CLR01, was recently reported to bind selectively to Lys side chains at the N-terminal region of αS and prevent its aggregation by electron-capture dissociation mass-spectrometry and PICUP study (Acharya *et al.* 2014). Using ThT fluorescence and EM, it is shown that in the presence of CLR01, αS did not form amyloid fibrils, and demonstrated that CLR01 inhibited αS-mediated toxicity in cell cultures and zebrafish embryos (Prabhudesai *et al.* 2012). The data of fluorescence and mass-spectrometric analysis suggested that CLR01 kept αS monomeric by increasing its reconfiguration rate (Acharya *et al.* 2014; Prabhudesai *et al.* 2012). It was shown that the polyphenol 3,4-dihydroxyphenylacetic acid (DOPAC) bound to the N-terminal region of αS and inhibited fibrillation of αS binding non-covalently (Zhou *et al.* 2009). By deleting residues 2-11 in the N-terminal, αS aggregation was delayed and cellular membrane permeabilization of αS monomer and oligomer could be abolished (Lorenzen *et al.*

2014a). It was shown that the N-terminal deletions in αS dramatically reduced toxicity towards yeast (Vamvaca *et al.* 2009). On the other hand, an NMR analysis revealed that EGCG noncovalently bound to C–terminal region of the monomeric αS (D119, S129, E130, and D135), and redirected αS into unstructured, off-pathway αS oligomers (Ehrnhoefer *et al.* 2008). EGCG did not affect oligomer size distribution or secondary structure, and rather, immobilized the C-terminal region and moderately reduced the degree of binding of oligomers to membrane (Lorenzen *et al.* 2014b). Based on the results of these studies (Acharya *et al.* 2014; Prabhudesai *et al.* 2012; Zhou *et al.* 2009; Lorenzen *et al.* 2014a; Vamvaca *et al.* 2009) and our NMR study, the binding region of αS with phenolic compounds might make equilibrium shift of αS aggregation capacities among the N-terminal, NAC, and the C-terminal region toward the suppression of aggregation. Interestingly, the anti-oligomerization effects of phenolic compounds on αS are similar to those on Aβ in our previous study (Ono *et al.* 2012a). In our previous NMR study with Aβ, Myr showed binding to monomeric Aβ at Arg-5, Ser-8, Gly-9, His-13, Lys-16, Asp-23, and Ile-31 (Ono *et al.* 2012a). There were no common amino acid sequences in Myr binding sites between Aβ and αS. Unlike the result of Myr, we found no direct binding of RA to monomeric αS in NMR study. In contrast, a previous NMR study reported the interaction between αS and RA, indicating that residues 3-18 and 38-51 of αS acted as noncovalent binding sites for RA (Rao *et al.* 2008). The discrepancy between the previous study (Rao *et al.* 2008) and the present study might be related to the lower concentration of αS used in the present study.

The ability of Myr and RA to block formation of low-order αS oligomers in our study is valuable, because low-order αS oligomers were thought to be the proximate neurotoxins in α-synucleinopathies from the results of several *in vitro* and *in vivo* studies (Outeiro *et al.* 2008; Paleologou *et al.* 2009; Tsigelny *et al.* 2008). Visualization of αS oligomerization in living cells using bimolecular fluorescence complementation revealed that formation of oligomeric αS species was a central step toward cytotoxicity, which can be targeted through the activity of molecular chaperones, such as heat shock protein 70 (Outeiro *et al.* 2008). Consistent with this result, toxicity was seen without heavily aggregated αS in the experiment of dopaminergic and non-dopaminergic neurons, and it has been suggested that soluble species mediate toxicity (Xu *et al.* 2002). We took into consideration these cumulative evidences, and performed LTP assay of hippocampal slices to evaluate synaptic toxicities induced by αS oligomers. LTP has been widely used as a neurophysiological model of activity-dependent synaptic plasticity, and are considered as important neurophysiological models of learning and memory (Martin *et al.* 2000). It has been reported that human Aβ oligomers inhibit hippocampal LTP *in vitro* and *in vivo* in rats (Townsend *et al.* 2006). However, knowledge about the effects of αS oligomers on synaptic plasticity is currently limited. It was reported that the exposure to αS oligomers impaired LTP through NMDA receptor activation, triggering enhanced contribution of calcium-permeable AMPA receptors in rat hippocampus slices (Dióogenes *et al.* 2012). The application of extracellular αS oligomers was reported to induce LTP suppression in hippocampal neurons via a calcineurin-dependent mechanism (Martin *et al.* 2012). Our work was consistent with previous studies (Martin *et al.* 2012; Dióogenes *et al.* 2012), where αS oligomers, not monomers, suppressed LTP in the hippocampal CA1 subfield, suggesting that memory formation is disturbed by αS oligomers. In contrast, cross-linked αS treated with Myr or RA partly cured LTP suppression. This result suggests that Myr and RA have preventive effects on αS oligomer-induced synaptic dysfunction by interfering with αS oligomerization. In recent studies, Cur showed effectiveness on motor activity, lifespan, oxidative stress, and apoptosis in the transgenic Drosophila model of Parkinson's disease (Siddique *et al.* 2013; Siddique *et al.* 2014). *In vivo* experiments with animal models of α-synucleinopathies should be conducted to elucidate the effectiveness of phenolic compounds on α-synucleinopathies.

To develop the therapies for α-synucleinopathies by phenolic compounds, we need to overcome several issues. The first issue is low bioavailability of phenolic compounds. Cur displayed low oral bioavailability, poor water-solubility, short biological half-life, and lower permeability through the brain blood barrier (BBB) (Anand *et al.* 2007). According to the data of clinical trial of Cur, bioavailability of Cur was not high; the range for serum concentration was between 0.51 ± 0.11 μM at a dose of 4000 mg/day and 1.77 ± 1.87 μM at a dose of 8000 mg/day (Cheng *et al.* 2001). A dose escalation study showed the safety of Cur intake in healthy volunteers, thus they took oral Cur ranged from 500 to 12000 mg and serious adverse events were not reported (Lao *et al.* 2006). To our best knowledge, there have been no reports about the orally-ingested Cur concentrations in cerebrospinal fluid. We have insufficient knowledge about bioavailability of Myr and RA, and we need to obtain further information about bioavailability of phenolic compounds. The next issue is the possibility that phenolic compounds may affect physiological functions of αS at synapses. Further experiments are necessary to elucidate whether extracellular phenolic compounds or intracellular phenolic compounds taken into the cell alter the synaptic functions. Specific targeting of extracellular αS has an additional advantage as a therapeutic strategy, as this approach will not interfere with the normal function of intracellular αS. Although the most of αS, a neuronal presynaptic protein, exists intracellularly, the secreted extracellular αS, particularly in oligomerized forms, was reported to play important roles in major pathological changes of α-synucleinopathies: deposition and spreading of aggregates, neuroinflammation, and neurodegeneration (Lee *et al.* 2014). We speculate that anti-oligomerization effects of phenolic compounds, such as Myr and RA, might reduce the formation of extracellular αS oligomers as well as intracellular αS oligomers, resulting in favorable effects on α-synucleinopathies.

In conclusion, our data established that the phenolic compounds inhibit oligomerization and statistical coils → β-sheet conversion of αS through different αS binding, and reduce αS oligomer-induced synaptic toxicity. Although the exact *in vivo* mechanisms underlying the benefits of polyphenols remain to be established, the present data, coupled with previously reported antioxidant and neuroprotective effects, suggest that phenolic compounds would be considerable candidates of disease modifying therapies for α-synucleinopathies.

Acknowledgments and conflict of interest disclosure

This work was supported by a grant for the Hokuriku Innovation Cluster for Health Science (M.Y.) and a Grant-in-Aid for Scientific Research (C) (26461266) (K.O.) from the Ministry of Education, Culture, Sports, Science and Technology, Japan, a grant for the Amyloidosis Research Committee (M.Y.) from the Ministry of Health, Labour, and Welfare, Japan, a grant from Takeda Science Foundation (K.O.), and a grant from Life Science Foundation of Japan (K.O.). No potential conflicts of interest were disclosed.

References

Acharya S., Safaie B. M., Wongkongkathep P., Ivanova M. I., Attar A., Klärner F. G., Schrader T., Loo J. A., Bitan G., and Lapidus L. J. (2014) Molecular basis for preventing α-synuclein aggregation by a molecular tweezer. *J. Biol. Chem.* **289**, 10727-10737.

Anand P., Kunnumakkara A. B., Neuman R. A., and Aggarwal B. B. (2007) Bioavailability of curcumin: problems and promises. *Mol. Pharm.* **4**, 807-818.

Ascherio A., Zhang S. M., Hernan M. A., Kawachi I., Colditz G. A., Speizer F. E., and Willett W. C. (2001) Prospective study of caffeine consumption and risk of Parkinson's disease in men and women. *Ann. Neurol.* **50**, 56-63.

Bieschke J., Russ J., Friedrich R. P., Ehrnhoefer D. E., Wobst H., Neugebauer K., and Wanker E. E. (2010) EGCG remodels mature α-synuclein and amyloid-β fibrils and reduces cellular toxicity. *Proc. Natl. Acad. Sci. USA.* **107**, 7710-7715.

Bitan G., and Teplow D. B. (2004) Rapid photochemical cross-linking--a new tool for studies of metastable, amyloidogenic protein assemblies. *Acc. Chem. Res.* **37**, 357-364.

Bosetti C., Spertini L., Parpinel M., Gnagnarella P., Lagiou P., Negri E., Franceschi S., Montella M., Peterson J., Dwyer J., Giacosa A., and La Vecchia C. (2005) Flavonoids and breast cancer risk in Italy. *Cancer Epidemiol. Biomarkers Prev.* **14**, 805-808.

Braak H., Ghebremedhin E., Rüb U., Bratzke H., and Del Tredici K. (2004) Stages in the development of Parkinson's disease-related pathology. *Cell Tissue Res.* **318**, 121-134.

Chan D. K., Woo J., Ho S. C., Pang C. P., Law L. K., Ng P. W., Hung W. T., Kwok T., Hui E., Orr K., Leung M. F., and Kay R. (1998) Genetic and environmental risk factors for Parkinson's disease in a Chinese population. *J. Neurol. Neurosurg. Psychiatry* **65**, 781-784.

Chao J., Leung Y., Wang M., and Chang R. C. (2012) Nutraceuticals and their preventive or potential therapeutic value in Parkinson's disease. *Nutr. Rev.* **70**, 373-386.

Cheng A. L., Hsu C. H., Lin J. K., Hsu M. M., Ho Y. F., Shen T. S., Ko J. Y., Lin J. T., Lin B. R., Ming-Shiang W., Yu H. S., Jee S. H., Chen G. S., Chen T. M., Chen C. A., Lai M. K., Pu Y. S., Pan M. H., Wang Y. J., Tsai C. C., and Hsieh C. Y. (2001) Phase I clinical trial of curcumin, a chemopreventive agent, in patients with high-risk or pre-malignant lesions. *Anticancer Res.* **21**, 2895-2900.

Clayton D. F., and George J. M. (1999) Synucleins in synaptic plasticity and neurodegenerative disorders. *J. Neurosci. Res.* **58**, 120-129.

Clubb R., Thanabal V., and Wagner G. (1992) A constant-time three-dimensional triple-rosonance pulse scheme to correlate intraresidue 1HN, 15N, and 13C' chemical shifts in 15N-13C-labelled proteins. *J. Magn. Reson.* **97**, 213-217.

Delaglio F., Grzesiek S., Vuister G. W., Zhu G., Pfeifer J., and Bax A. (1995) NMRPipe: a multidimensional spectral processing system based on UNIX pipes. *J. Biomol. NMR* **6**, 277-293.

Diógenes M. J., Dias R. B., Rombo D. M., Vicente Miranda H., Maiolino F., Guerreiro P., Näsström T., Franquelim H. G., Oliveira L. M., Castanho M. A., Lannfelt L., Bergström J., Ingelsson M., Quintas A., Sebastião A. M., Lopes L. V., and Outeiro T. F. (2012) Extracellular α-synuclein oligomers modulate synaptic transmission and impair LTP via NMDA-receptor activation. *J. Neurosci.* **32**, 11750-11762.

Ehrnhoefer D. E., Bieschke J., Boeddrich A., Herbst M., Masino L., Lurz R., Engemann S., Pastore A., and Wanker E. E. (2008) EGCG redirects amyloidogenic polypeptides into unstructured, off-pathway oligomers. *Nat. Struct. Mol. Biol.* **15**, 558-566.

Fancy D. A., and Kodadek T. (1999) Chemistry for the analysis of protein-protein interactions: rapid and efficient cross-linking triggered by long wavelength light. *Proc. Natl. Acad. Sci. USA.* **96**, 6020-6024.

Fujiwara H., Hasegawa M., Dohmae N., Kawashima A., Masliah E., Goldberg M. S., Shen J., Takio K., and Iwatsubo T. (2002) α-Synuclein is phosphorylated in synucleinopathy lesions. *Nat. Cell. Biol.* **4**, 160-164.

Gao X., Cassidy A., Schwarzschild M. A., Rimm E. B., and Ascherio A. (2012) Habitual intake of dietary flavonoids and risk of Parkinson disease. *Neurology* **78**, 1138-1145.

Grzesiek S., and Bax A. (1992a) Improved 3D triple resonance NMR techniques applied to a 31 kDa protein. *J. Magn. Reson.* **96**, 432-440.

Grzesiek S., and Bax A. (1992b) An efficient for sequential backbone assignment of medium sized isotopically enriched proteins. *J. Magn. Reson.* **99**, 201-207.

Grzesiek S., and Bax A. (1993) Amino acid type determination in the sequential assignment procedure of uniformly 13C/15N-enriched proteins. *J. Biomol. NMR* **3**, 185-204.

Hejjaoui M., Butterfield S., Fauvet B., Vercruysse F., Cui J., Dikiy I., Prudent M., Olschewski D., Zhang Y., Eliezer D., and Lashuel H. A. (2012) Elucidating the role of C-terminal post-translational modifications using protein semisynthesis strategies: α-synuclein phosphorylation at tyrosine 125. *J. Am. Chem. Soc.* **134**, 5196-5210.

Izawa Y., Tateno H., Kameda H., Hirakawa K., Hato K., Yagi H., Hongo K., Mizobata T., and Kawata Y. (2012) Role of C-terminal negative charges and tyrosine residues in fibril formation of α-synuclein. *Brain Behav.* **2**, 595-605.

Jankovic J. (2008) Parkinson's disease: clinical features and diagnosis. *J. Neurol. Neurosurg. Psychiatry* **79**, 368-376.

Jiang T. F., Zhang Y. J., Zhou H. Y., Wang H. M., Tian L. P., Liu J., Ding J. Q., and Chen S. D. (2013) Curcumin Ameliorates the Neurodegenerative Pathology in A53T α-synuclein Cell Model of Parkinson's Disease Through the Downregulation of mTOR/p70S6K Signaling and the Recovery of Macroautophagy. *J. Neuroimmune Pharmacol.* **8**, 356-369.

Johnson B. A. (2004) Using NMRView to visualize and analyze the NMR spectra of macromolecules. *Methods Mol. Biol.* **278**, 313-352.

Lao C. D., Ruffin M. T. 4th., Normolle D., Heath D. D., Murray S. I., Bailey J. M., Boggs M. E., Crowell J., Rock C. L., and Brenner D. E. (2006) Dose escalation of a curcuminoid formulation. BMC Complement. *Altern. Med.* **6**, 10.

Lee H. J., Bae E. J., nad Lee S. J. (2014) Extracellular α-synuclein-a novel and crucial factor in Lewy body diseases. *Nat. Rev. Neurol.* **10**, 92-98.

LeVine H., 3rd. (1993) Thioflavine T interaction with synthetic Alzheimer's disease β-amyloid peptides: detection of amyloid aggregation in solution. *Protein. Sci.* **2**, 404-410.

Levites Y., Weinreb O., Maor G., Youdim M. B., and Mandel S. (2001) Green tea polyphenol (-)-epigallocatechin-3-gallate prevents N-methyl-4-phenyl-1,2,3,6-tetrahydropyridine-induced dopaminergic neurodegeneration. *J. Neurochem.* **78**, 1073-1082.

Liu Z., Yu Y., Li X., Ross C. A., and Smith W. W. (2011) Curcumin protects against A53T α-synuclein-induced toxicity in a PC12 inducible cell model for Parkinsonism. *Pharmacol. Res.* **63**, 439-444.

Lorenzen N., Lemminger L., Pedersen J. N., Nielsen S. B., and Otzen D. E. (2014a) The N-terminus of α-synuclein is essential for both monomeric and oligomeric interactions with membranes. *FEBS Lett.* **588**, 497-502.

Lorenzen N., Nielsen S. B., Yoshimura Y., Vad B. S., Andersen C. B., Betzer C., Kaspersen J. D., Christiansen G., Pedersen J. S., Jensen P. H., Mulder F. A., and Otzen D. E. (2014b) How epigallocatechin gallate can inhibit α-synuclein oligomer toxicity in vitro. *J. Biol. Chem.* **289**, 21299-21310.

Martin S. J., Grimwood P. D., and Morris R. G. (2000) Synaptic plasticity and memory: an evaluation of the hypothesis. *Annu. Rev. Neurosci.* **23**, 649-711.

Martin Z. S., Neugebauer V., Dineley K. T., Kayed R., Zhang W., Reese L. C., and Taglialatela G. (2012) α-Synuclein oligomers oppose long-term potentiation and impair memory through a calcineurin-dependent mechanism: relevance to human synucleopathic diseases. *J. Neurochem.* **120**, 440-452.

Masuda M., Suzuki N., Taniguchi S., Oikawa T., Nonaka T., Iwatsubo T., Hisanaga S., Goedert M., and Hasegawa M. (2006) Small molecule inhibitors of α-synuclein filament assembly. *Biochemistry* **45**, 6085-6094.

McKeith I. G., Dickson D. W., Lowe J., Emre M., O'Brien J. T., Feldman H., Cummings J., Duda J. E., Lippa C., Perry E. K., Aarsland D., Arai H., Ballard C. G., Boeve B., Burn D. J., Costa D., Del Ser T., Dubois B., Galasko D., Gauthier S., Goetz C. G., Gomez-Tortosa E., Halliday G., Hansen L. A., Hardy J., Iwatsubo T., Kalaria R. N., Kaufer D., Kenny R. A., Korczyn A., Kosaka K., Lee V. M., Lees A., Litvan I., Londos E., Lopez O. L., Minoshima S., Mizuno Y., Molina J. A., Mukaetova-Ladinska E. B., Pasquier F., Perry R. H., Schulz J. B., Trojanowski J. Q., and Yamada M. (2005) Diagnosis and management of dementia with Lewy bodies: third report of the DLB Consortium. Neurology **65**, 1863-1872.

Naiki H., and Nakakuki K. (1996) First-order kinetic model of Alzheimer's β-amyloid fibril extension in vitro. *Lab. Invest.* **74**, 374-383.

Ono K., and Yamada M. (2006) Antioxidant compounds have potent anti-fibrillogenic and fibril-destabilizing effects for α-synuclein fibrils in vitro. *J. Neurochem.* **97**, 105-115.

Ono K., and Yamada M. (2011) Low-n oligomers as therapeutic targets of Alzheimer's disease. *J. Neurochem.* **117**, 19-28.

Ono K., Yoshiike Y., Takashima A., Hasegawa K., Naiki H., and Yamada M. (2003) Potent anti-amyloidogenic and fibril-destabilizing effects of polyphenols in vitro: implications for the prevention and therapeutics of Alzheimer's disease. *J. Neurochem.* **87**, 172-181.

Ono K., Condron M. M., Ho L., Wang J., Zhao W., Pasinetti G. M., and Teplow D. B. (2008) Effects of grape seed-derived polyphenols on amyloid β-protein self-assembly and cytotoxicity. *J. Biol. Chem.* **283**, 32176-32187.

Ono K., Ikeda T., Takasaki J., and Yamada M. (2011) Familial Parkinson disease mutations influence α-synuclein assembly. *Neurobiol. Dis.* **43**, 715-724.

Ono K., Li L., Takamura Y., Yoshiike Y., Zhu L., Han F., Mao X., Ikeda T., Takasaki J., Nishijo H., Takashima A., Teplow D. B., Zagorski M. G., and Yamada M. (2012a) Phenolic compounds prevent amyloid β-protein oligomerization and synaptic dysfunction by site-specific binding. *J. Biol. Chem.* **287**, 14631-14643.

Ono K., Mochizuki H., Ikeda T., Nihira T., Takasaki J., Teplow D. B., and Yamada M. (2012b) Effect of melatonin on α-synuclein self-assembly and cytotoxicity. *Neurobiol. Aging* **33**, 2172-2185.

Ono K., Takasaki J., Takahashi R., Ikeda T., and Yamada M. (2013) Effects of antiparkinsonian agents on β-amyloid and α-synuclein oligomer formation in vitro. *J. Neurosci. Res.* **91**, 1371-1381.

Outeiro T. F., Putcha P., Tetzlaff J. E., Spoelgen R., Koker M., Carvalho F., Hyman B. T., and McLean P. J. (2008) Formation of toxic oligomeric α-synuclein species in living cells. *PLoS One* **3**, e1867.

Paleologou K. E., Kragh C. L., Mann D. M., Salem S. A., Al-Shami R., Allsop D., Hassan A. H., Jensen P. H., and El-Agnaf O. M. (2009) Detection of elevated levels of soluble α-synuclein oligomers in post-mortem brain extracts from patients with dementia with Lewy bodies. *Brain* **132**, 1093-1101.

Prabhudesai S., Sinha S., Attar A., Kotagiri A., Fitzmaurice A. G., Lakshmanan R., Ivanova M. I., Loo J. A., Klärner F. G., Schrader T., Stahl M., Bitan G., and

Bronstein J. M. (2012) A novel "molecular tweezer" inhibitor of α-synuclein neurotoxicity in vitro and in vivo. *Neurotherapeutics* **9**, 464-476.

Rao J. N., Dua V., and Ulmer T. S. (2008) Characterization of α-synuclein interactions with selected aggregation-inhibiting small molecules. *Biochemistry* **47**, 4651-4656.

Rao J. N., Kim Y. E., Park L. S., and Ulmer, T. S. (2009) Effect of pseudorepeat rearrangement on α-synuclein misfolding, vesicle binding, and micelle binding. *J. Mol. Biol.* **390**, 516-529.

Shen Y., Lange O., Delaglio F., Rossi P., Aramini J. M., Liu G., Eletsky A., Wu Y., Singarapu K. K., Lemak A., Ignatchenko A., Arrowsmith C. H., Szyperski T., Montelione G. T., Baker D., and Bax A. (2008) Consistent blind protein structure generation from NMR chemical shift data. *Proc. Natl. Acad. Sci. USA.* **105**, 4685-4690.

Shen Y., Vernon R., Baker D., and Bax A. (2009) De novo protein structure generation from incomplete chemical shift assignments. *J. Biomol. NMR* **43**, 63-78.

Siddique Y. H., Khan W., Singh B. R., and Naqvi A. H. (2013) Synthesis of alginate-curcumin nanocomposite and its protective role in transgenic Drosophila model of Parkinson's disease. *ISRN Pharmacol.* **2013**, 794582.

Siddique Y. H., Naz F., and Jyoti S. (2014) Effect of curcumin on lifespan, activity pattern, oxidative stress, and apoptosis in the brains of transgenic Drosophila model of Parkinson's disease. *Biomed. Res. Int.* **2014**, 606928.

Spillantini M. G., Crowther R. A., Jakes R., Hasegawa M., and Goedert M. (1998) α-synuclein in filamentous inclusions of Lewy bodies from Parkinson's disease and dementia with lewy bodies. *Proc. Natl. Acad. Sci. USA.* **95**, 6469-6473.

Takamura Y., Ono K., Matsumoto J., Yamada M., and Nishijo H. (2014) Effects of the neurotrophic agent T-817MA on oligomeric amyloid-β-induced deficits in long-term potentiation in the hippocampal CA1 subfield. *Neurobiol. Aging* **35**, 532-536.

Townsend M., Shankar G. M., Mehta T., Walsh D. M., and Selkoe D. J. (2006) Effects of secreted oligomers of amyloid β-protein on hippocampal synaptic plasticity: a potent role for trimers. *J. Physiol.* **572**, 477-492.

Tsigelny I. F., Crews L., Desplats P., Shaked G. M., Sharikov Y., Mizuno H., Spencer B., Rockenstein E., Trejo M., Platoshyn O., Yuan J. X., and Masliah E. (2008) Mechanisms of hybrid oligomer formation in the pathogenesis of combined Alzheimer's and Parkinson's diseases. *PLoS One* **3**, e3135.

Uversky V. N., Lee H. J., Li J., Fink A. L., and Lee S. J. (2001) Stabilization of partially folded conformation during α-synuclein oligomerization in both purified and cytosolic preparations. *J. Biol. Chem.* **276**, 43495-43498.

Vamvaca K., Volles M. J., and Lansbury P. T., Jr. (2009) The first N-terminal amino acids of α-synuclein are essential for α-helical structure formation in vitro and membrane binding in yeast. *J. Mol. Biol.* **389**, 413-424.

Volles M. J., Lee S. J., Rochet J. C., Shtilerman M. D., Ding T. T., Kessler J. C., and Lansbury P. T., Jr. (2001) Vesicle permeabilization by protofibrillar α-synuclein: implications for the pathogenesis and treatment of Parkinson's disease. *Biochemistry* **40**, 7812-7819.

Weinreb P. H., Zhen W., Poon A. W., Conway K. A., and Lansbury P. T., Jr. (1996) NACP, a protein implicated in Alzheimer's disease and learning, is natively unfolded. *Biochemistry* **35**, 13709-13715.

Weinreb O., Amit T., Mandel S., and Youdim M. B. (2009) Neuroprotective molecular mechanisms of (-)-epigallocatechin-3-gallate: a reflective outcome of its antioxidant, iron chelating and neuritogenic properties. *Genes. Nutr.* **4**, 283-296.

Winner B., Jappelli R., Maji S. K., Desplats P. A., Boyer L., Aigner S., Hetzer C., Loher T., Vilar M., Campioni S., Tzitzilonis C., Soragni A., Jessberger S., Mira H., Consiglio A., Pham E., Masliah E., Gage F. H., and Riek R. (2011) In vivo demonstration that α-synuclein oligomers are toxic. *Proc. Natl. Acad. Sci. USA.* **108**, 4194-4199.

Wood S. J., Wypych J., Steavenson S., Louis J. C., Citron M., and Biere A. L. (1999) α-synuclein fibrillogenesis is nucleation-dependent. Implications for the pathogenesis of Parkinson's disease. *J. Biol. Chem.* **274**, 19509-19512.

Wu K. P., Kim S., Fela D. A., and Baum J. (2008) Characterization of conformational and dynamic properties of natively unfolded human and mouse α-synuclein ensembles by NMR: implication for aggregation. *J. Mol. Biol.* **378**, 1104-1115.

Xu J., Kao S. Y., Lee F. J., Song W., Jin L. W., and Yankner B. A. (2002) Dopamine-dependent neurotoxicity of α-synuclein: a mechanism for selective neurodegeneration in Parkinson disease. *Nat. Med.* **8**, 600-606.

Zhou W., Gallagher A., Hong D. P., Long C., Fink A. L., and Uversky V. N. (2009) At low concentrations, 3,4-dihydroxyphenylacetic acid (DOPAC) binds non-covalently to α-synuclein and prevents its fibrillation. *J. Mol. Biol.* **388**, 597-610.

Zhu M., Rajamani S., Kaylor J., Han S., Zhou F., and Fink A. L. (2004) The flavonoid baicalein inhibits fibrillation of α-synuclein and disaggregates existing fibrils. *J. Biol. Chem.* **279**, 26846-26857.

Figure Legends

Fig. 1. Chemical structures of Myr, FA, NDGA, Cur, and RA.

Fig. 2. αS and GST oligomerizations. PICUP, followed by SDS-PAGE and silver staining, was used to determine the effects of 25 and 250 μM Myr, FA, NDGA, Cur, or RA on oligomerization of αS (A) or GST (B). Consequently, we showed concentration dependent inhibitory effects of αS oligomerization of Myr (C) or RA (D). +, with cross-linking; -, without cross-linking. The gel is representative of each of three independent experiments.

Fig. 3. αS assembly morphology. AFM was performed on 25 μM uncross-linked (A) and cross-linked (B-G) αS without (B) or with 50 μM Myr (C), FA (D), NDGA (E), Cur (F), or RA (G). EM was performed on 25 μM uncross-linked (H) and cross-linked (I-N) αS without (I) or with 50 μM Myr (J), FA (K), NDGA (L), Cur (M), or RA (N). Scale bars indicate 100 nm.

Fig. 4. αS secondary structure dynamics. CD was used to monitor peptide assembly. 25 μM αS (A-C) were incubated at 37°C for 5 days in 20 mM Tris-HCl buffer, pH 7.4, in buffer alone (A) or in the presence of 50 μM Myr (B) or RA (C). Spectra were acquired immediately at the start of the incubation period, day 0 (○), and after days 1

(●), 2 (□), 3 (■), 4 (△), and 5 (▲). The spectra presented at each time are representative of those obtained during each of three independent experiments.

Fig. 5. Effects of Myr or RA on cross-linked αS-induced alterations of LTP in the hippocampal slices. **(**A) Synaptic toxicity. Typical fEPSP waveforms of pre- (black lines) and post-tetanic (dashed red lines) stimulation in each test group. Thirty waveforms were averaged. (B) Time course of %fEPSPs slope. Arrows indicate tetanus stimulation (100 Hz, 1 s, 2 train). (C) Values are shown as the percentage of fEPSP slope relative to the baseline and presented as mean ± S.E. Significant difference between cross-linked αS versus other experimental group, along with their associated *p*-values, where * signifies $p < 0.05$ and ** signifies $p < 0.01$

Fig. 6. Analysis of interaction between αS and polyphenols. (A, B) ^{1}H-^{15}N HSQC spectra of αS in the absence of (black contour) and in the presence of (red contour) polyphenols. (A) Myr and (B) RA. Residues with intensity ratios ($I_{\mathrm{bound}}/I_{\mathrm{free}}$) < 0.15 are labeled. An unassigned resonance is indicated by asterisk. (C, D) Model representation of αS that show binding locations with polyphenols. The red-colored regions are the residues that showed the peak broadening in the presence of polyphenols. (C) Myr and (D) RA.

Table 1. Morphological analysis of αS assemblies

Assembly	Diameter[a]	Height[b]
Uncross-linked αS	2.32 ± 0.17 (30)	0.53 ± 0.05 (30)
Cross-linked αS	11.94 ± 1.51 (30)	1.60 ± 0.24 (30)
Cross-linked αS with Myr	2.80 ± 0.34 (30)	0.58 ± 0.06 (30)
Cross-linked αS with NDGA	2.70 ± 0.27 (30)	0.54 ± 0.06 (30)
Cross-linked αS with FA	2.99 ± 0.38 (30)	0.57 ± 0.07 (30)
Cross-linked αS with Cur	3.15 ± 0.38 (30)	0.60 ± 0.07 (30)
Cross-linked αS with RA	2.67 ± 0.35 (30)	0.57 ± 0.06 (30)

[a] Mean diameter ± SE, in nanometers, is listed for (n) αS assemblies visualized by EM.

[b] Mean diameter ± SE, in nanometers, is listed for (n) αS assemblies visualized by AFM.

Supporting information

Figure S1. Size exclusion chromatography (SEC) of αS assemblies. SEC was performed on 25 μM cross-linked αS without phenolic compound (A), or with 50 μM Myr (B) or RA (C) for removing reagents. Fractions were lyophilized immediately after collection. Lyophilization and reconstitution did not alter the oligomer composition of any of the peptide populations under study (D). Lanes 1-2 showed pre-SEC state of uncross-linked and cross-linked αS. Lanes 3, 5, and 7 showed pre-SEC state, and Lanes 4, 6, and 8 showed post-SEC state of cross-linked αS without or with Myr or RA, respectively.

Figure S2. The secondary structures and seeding activities of αS assemblies. CD was used to measure the secondary structure of 25 μM uncross-linked αS (○; UnXL), cross-linked αS without (●; XL), or with 50 μM Myr (□; XL+Myr) or RA (×; XL+RA) (A). 10% (v/v) uncross-linked (○; UnXL), or 25 μM cross-linked αS without (●; 10% XL) or with Myr (□; 10% XL+Myr) or RA (×; 10% XL+RA) was added to un cross-linked αS, which then was incubated for 24-168 hr at 37°C in 20 mM Tris buffer, pH 7.4. Aliquots were assayed periodically using ThS. Binding is expressed as mean fluorescence (in arbitrary fluorescence units [FU]) ± SE. ThS fluorescence were measured at 0, 1, 2, 6, 24. 48, 72, 96, 120, 144, and 168 hrs. Data was obtained in three independent experiments (B).

Fig. 1

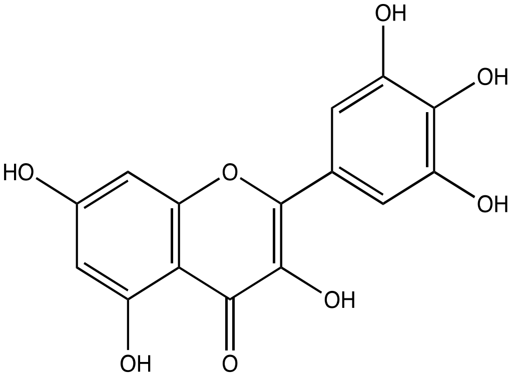

Myr

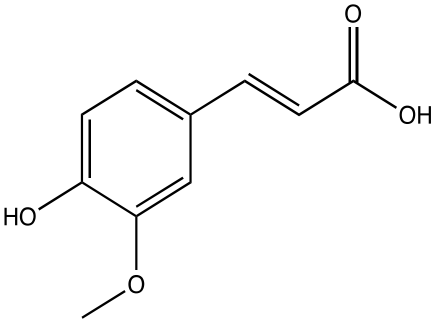

FA

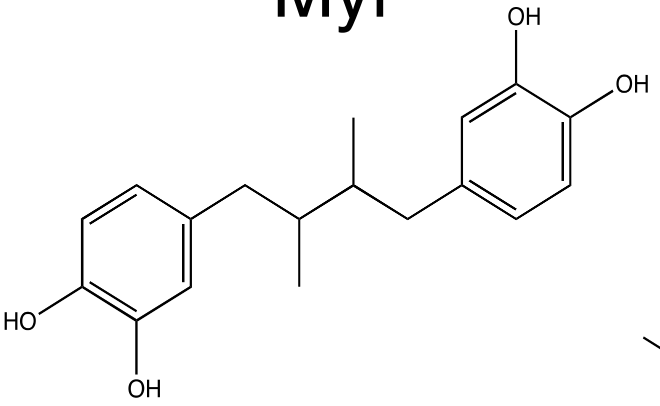

NDGA

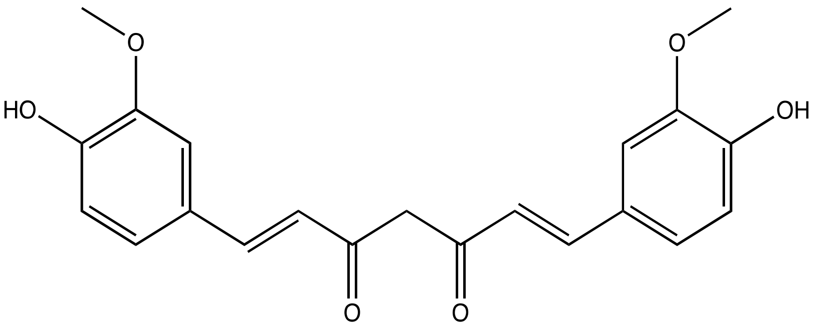

Cur

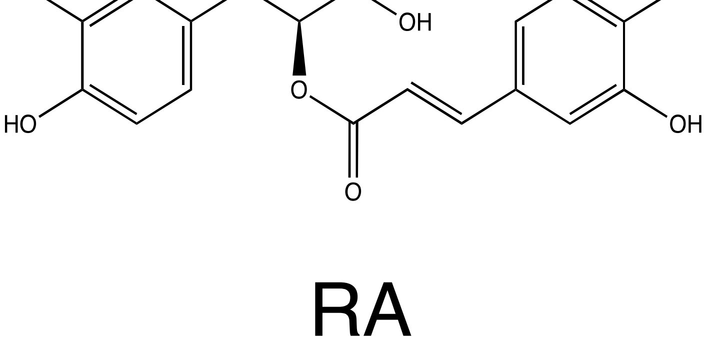

RA

Fig. 2

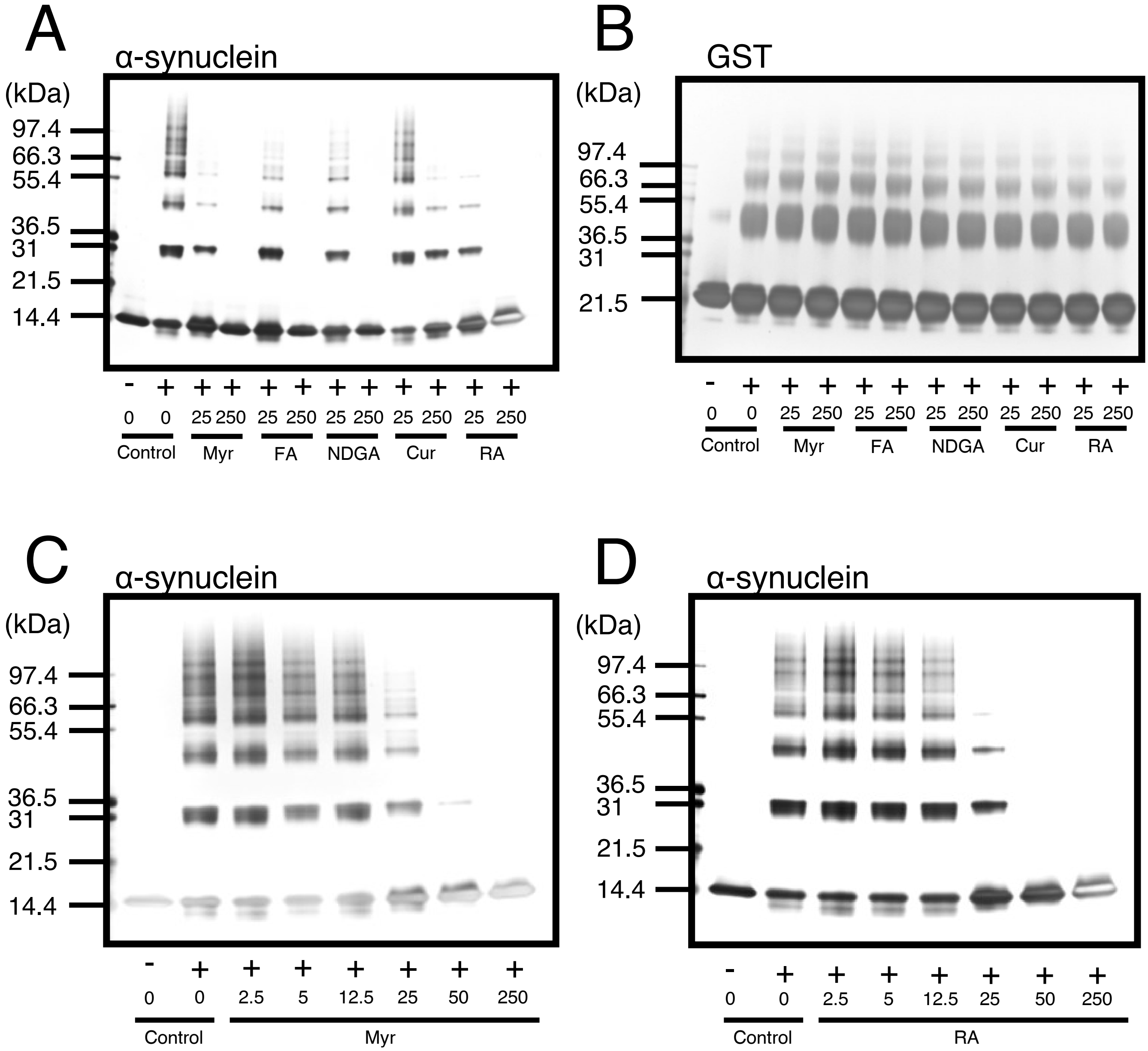
A
α-synuclein
(kDa)
97.4
66.3
55.4
36.5
31
21.5
14.4
- + + + + + + + + + + +
0 0 25 250 25 250 25 250 25 250 25 250
Control
Myr
FA
NDGA
Cur
RA
B
GST
(kDa)
97.4
66.3
55.4
36.5
31
21.5
- + + + + + + + + + + +
0 0 25 250 25 250 25 250 25 250 25 250
Control
Myr
FA
NDGA
Cur
RA
C
α-synuclein
(kDa)
97.4
66.3
55.4
36.5
31
21.5
14.4
- + + + + + + +
0 0 2.5 5 12.5 25 50 250
Control
Myr
D
α-synuclein
(kDa)
97.4
66.3
55.4
36.5
31
21.5
14.4
- + + + + + + +
0 0 2.5 5 12.5 25 50 250
Control
RA

Fig. 3

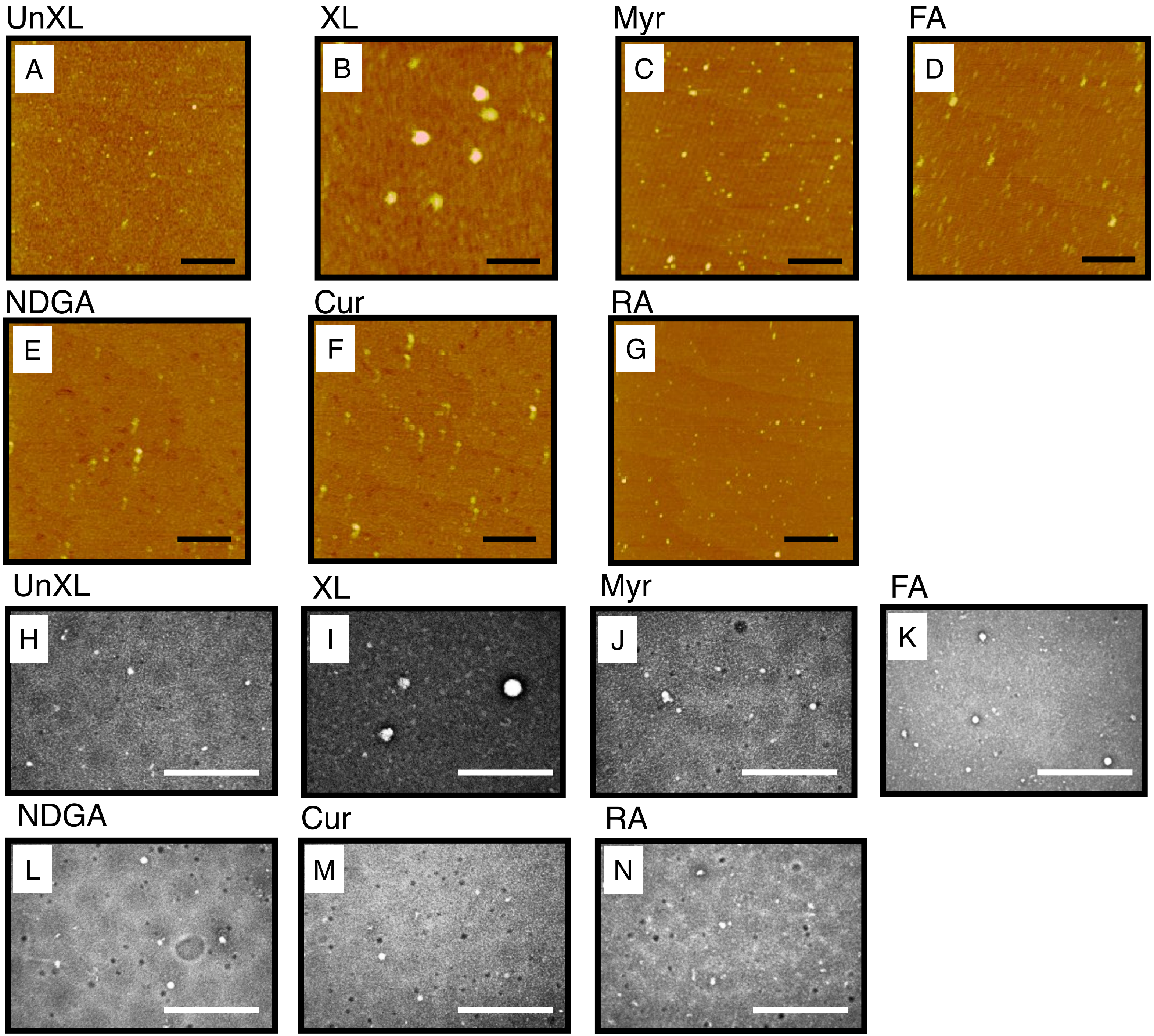
UnXL
A
XL
B
Myr
C
FA
D
NDGA
E
Cur
F
RA
G
UnXL
H
XL
I
Myr
J
FA
K
NDGA
L
Cur
M
RA
N

Fig. 4

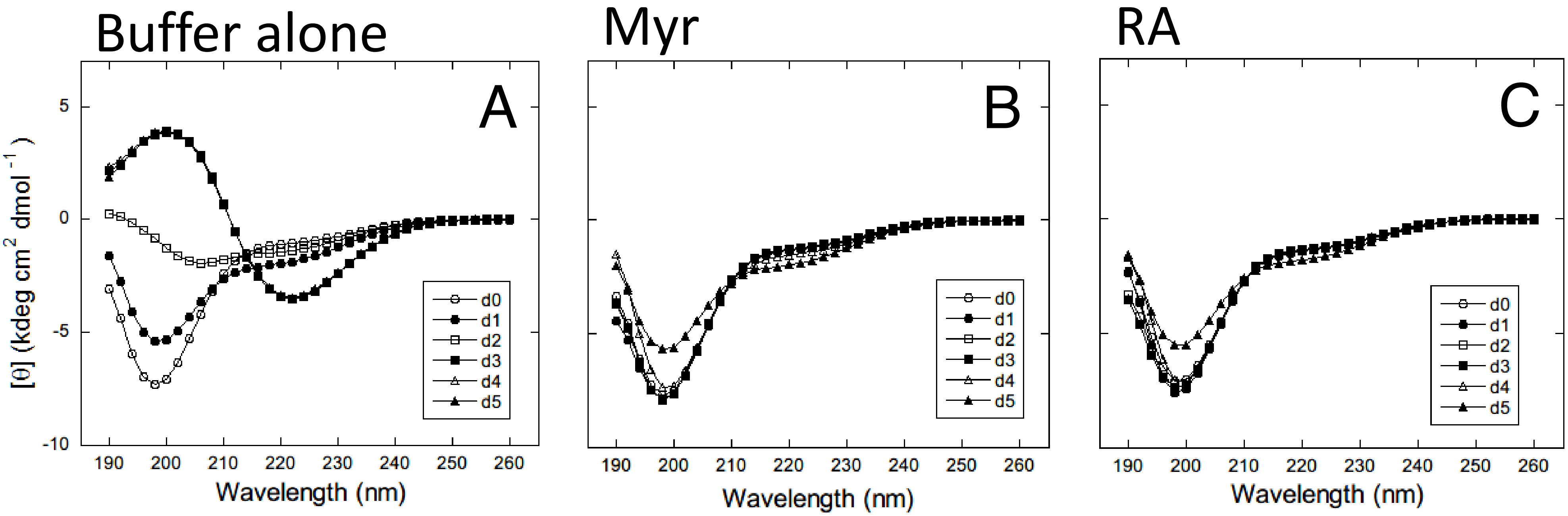
Buffer alone

Myr

RA

Fig. 5

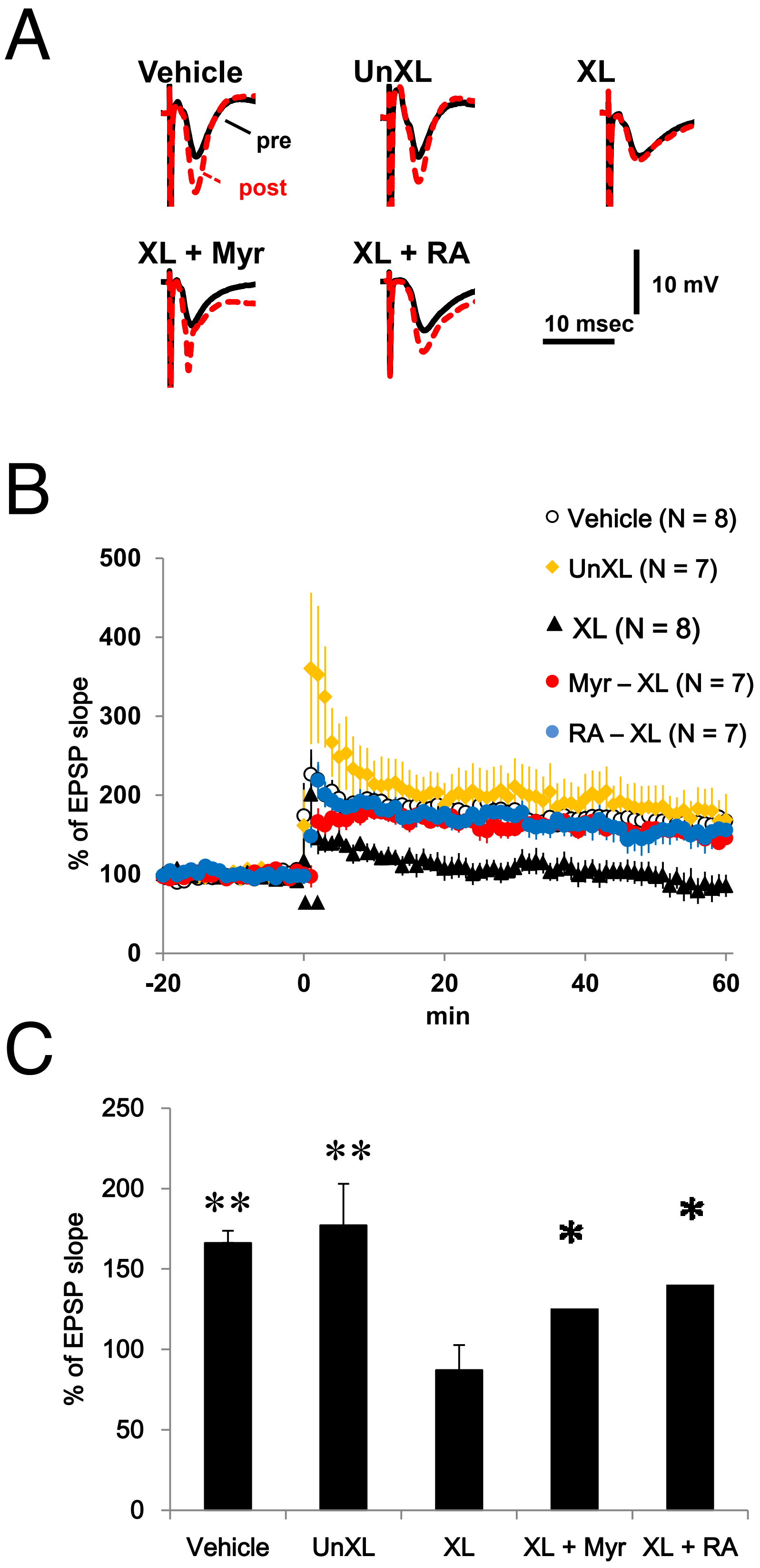
A
Vehicle
pre
post
UnXL
XL
XL + Myr
XL + RA
10 mV
10 msec
B
○ Vehicle (N = 8)
◆ UnXL (N = 7)
▲ XL (N = 8)
● Myr – XL (N = 7)
● RA – XL (N = 7)
% of EPSP slope
500
400
300
200
100
0
-20
0
20
40
60
min
C
% of EPSP slope
250
200
150
100
50
0
**
**
*
*
Vehicle
UnXL
XL
XL + Myr
XL + RA

Fig. 6

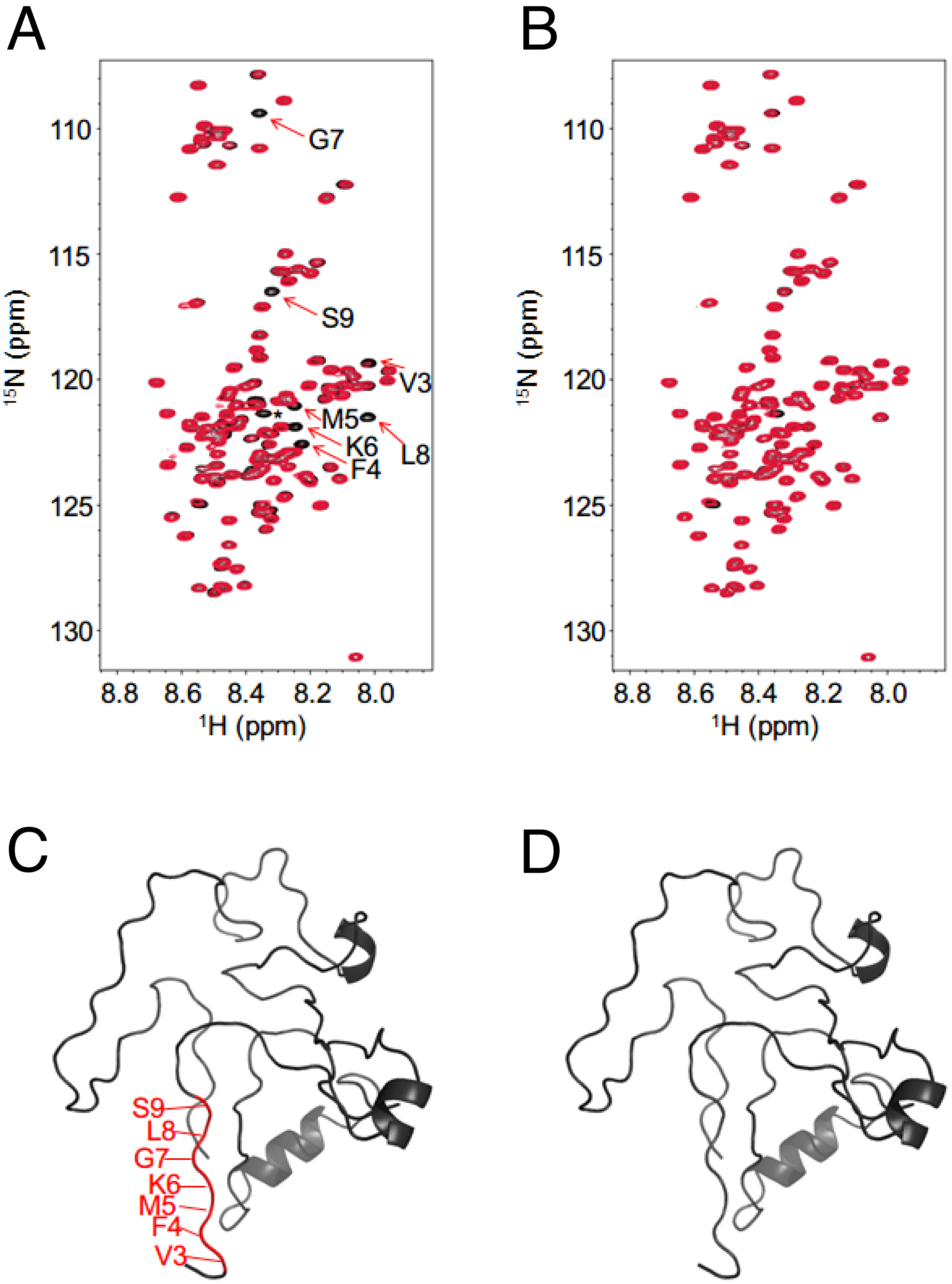
A
B
110
115
120
125
130
^{15}N (ppm)
8.8
8.6
8.4
8.2
8.0
^{1}H (ppm)
G7
S9
V3
M5
K6
L8
F4
*
C
D
S9
L8
G7
K6
M5
F4
V3

Figure S1

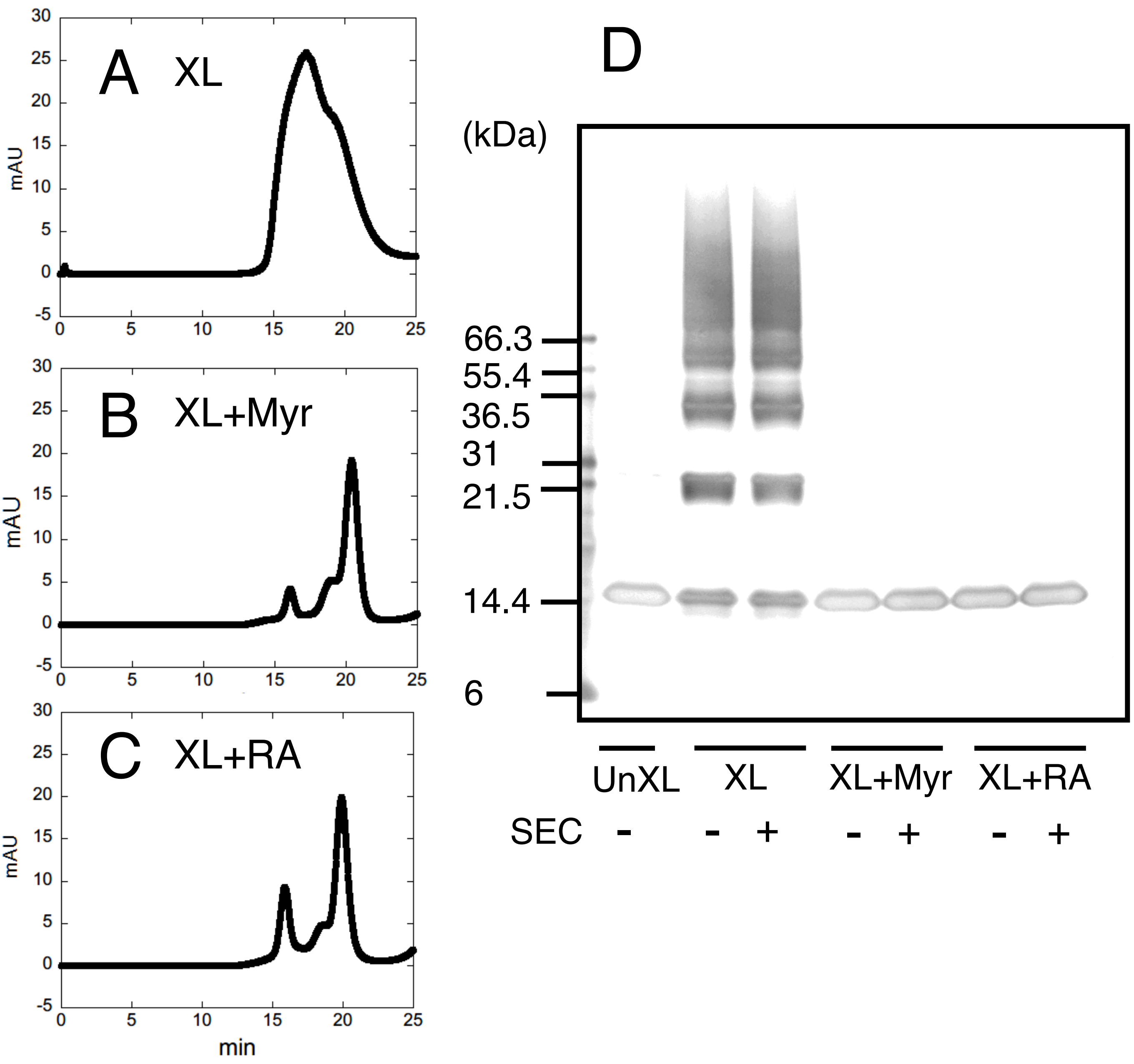
A
XL
B
XL+Myr
C
XL+RA
mAU
30
25
20
15
10
5
0
-5
0
5
10
15
20
25
min
D
(kDa)
66.3
55.4
36.5
31
21.5
14.4
6
UnXL
XL
XL+Myr
XL+RA
SEC
-
-
+
-
+
-
+

Figure S2

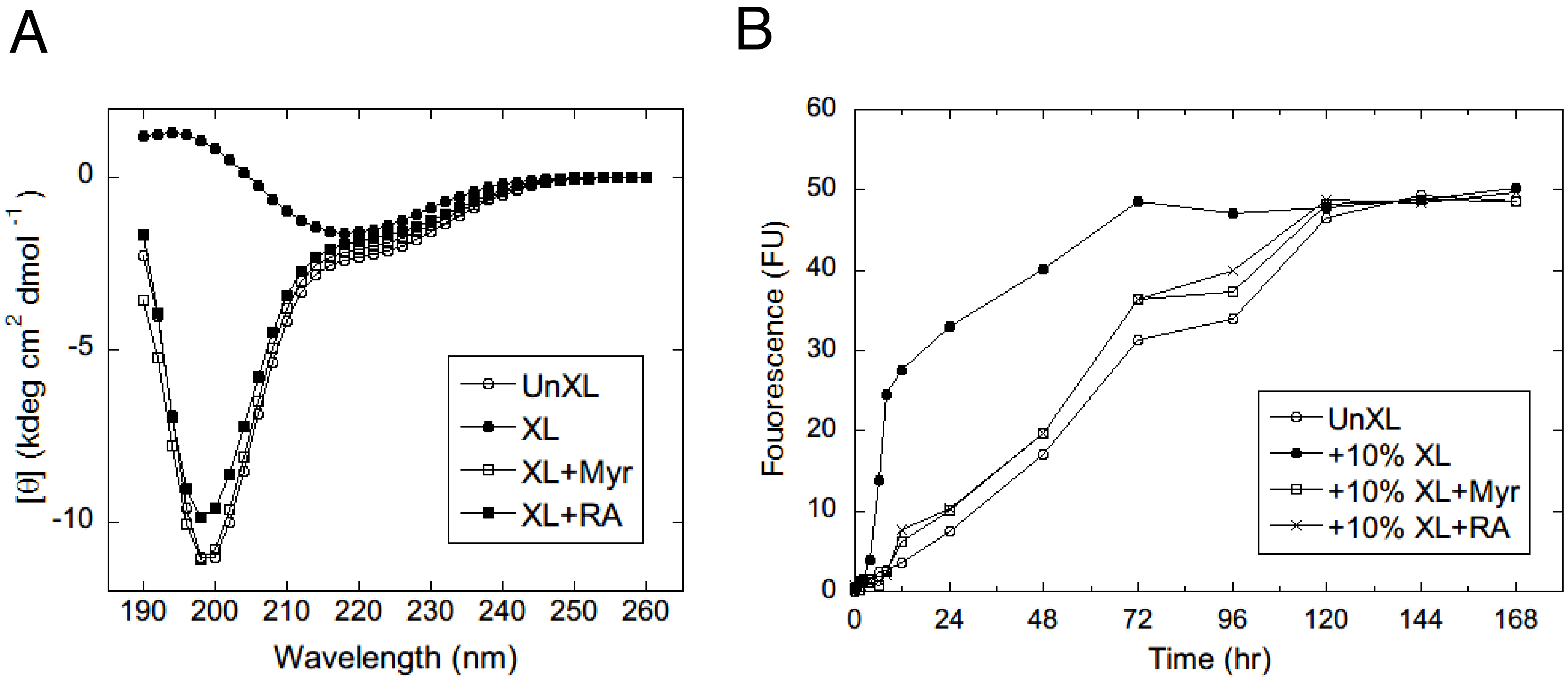
A
0
-5
-10
[θ] (kdeg cm^2 dmol^{-1})
190
200
210
220
230
240
250
260
Wavelength (nm)
UnXL
XL
XL+Myr
XL+RA
B
60
50
40
30
20
10
0
Fouorescence (FU)
0
24
48
72
96
120
144
168
Time (hr)
UnXL
+10% XL
+10% XL+Myr
+10% XL+RA